Scheme I

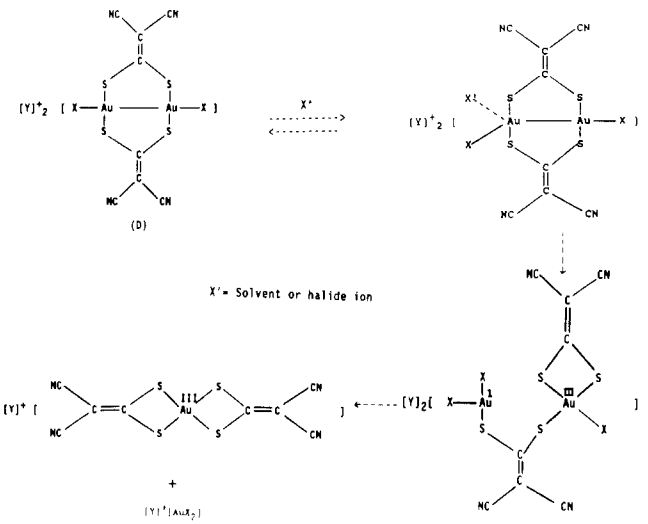

the gold center destabilizes the dimer. With the gold(II) ylide complex, $Au_2(ylide)_2Cl_2$, ligand rearrangement occurs[9c,22] in an ionizing solvent to form the mixed-valent Au^{III}/Au^{I} species Cl(ylide)Au^{III}(ylide)Au^{I}Cl. Rupture of the Au–Au bond is required. Thus, a nucleophilic solvent, or nucleophiles in general, appear to destabilize the metal–metal bond in these d^9–d^9 dimer systems.

Stated differently, the important step in the homovalent Au^{II}_2 to the hetervalent Au^{III}/Au^{I} rearrangement is an association of either halide ions or a solvent molecule to form a 5-coordinate Au^{II} center, as is shown in Scheme I. Rupture of the metal–metal bond and a metal–ligand bond allows rearrangement of the molecule to a 3-coordinate Au^{I} and a 4-coordinate Au^{III} center via ligand addition to the latter. The formation of 3-coordinate Au^{I} and 4-coordinate planar Au^{III} is very common.[23,16] The labile sulfur compounds further rearrange to stable mononuclear planar Au^{III} and linear Au^{I} species.

In summary, strong σ-donor ligands support the electrophilic excitation of the d^{10} configuration to a d^9s^1 configuration, thus forming a stable metal–metal-bonded Au^{II} system with oxidative addition across the two metal atoms. In this *i*-MNT system the dianionic nature of the ligand coordinated through the sulfur atoms supplies sufficient electron density through σ donation to the Au^{I} centers to form a stable Au^{II} product. The stability of the Au^{II} product is dependent on the nature of halogen used as an oxidant. The rate of disproportionation of $[Y^+]_2[Au_2(i\text{-}MNT)_2X_2]$ is dependent on halide ion concentration as well as coordinating solvents. Decomposition occurs by a pseudo-first-order reaction pathway in the absence of excess halide.

Acknowledgment. This work has been supported by the National Science Foundation (Grant CHE 8708725), the Robert A. Welch Foundation, and the Texas A&M University Available Fund.

Supplementary Material Available: For **1a–4**, listings of crystallographic data, anisotropic thermal parameters, H atom coordinates, and isotropic thermal parameters (11 pages); tables of F_o, F_c, and $\sigma(F)$ (119 pages). Ordering information is given on any current masthead page.

Contribution from the Departments of Chemistry, Faculty of Engineering Science, Osaka University, Toyonaka, Osaka 560, Japan, and Faculty of Science, Yamagata University, Yamagata 990, Japan

Synthesis, Structure, and Electronic Properties of Octakis(μ_3-sulfido)hexakis(triethylphosphine)hexatungsten as a Tungsten Analogue of the Molecular Model for Superconducting Chevrel Phases

Taro Saito,*,† Akihiko Yoshikawa,† Tsuneaki Yamagata,† Hideo Imoto,† and Kei Unoura‡

Received February 3, 1989

The hexanuclear tungsten complex $[W_6S_8(PEt_3)_6]$ was synthesized by the reaction of magnesium metal on a trinuclear tungsten chloro sulfido cluster compound prepared from W_6Cl_{12}, elemental sulfur, and triethylphosphine. The complex crystallizes in the triclinic space group $P\bar{1}$ with a = 20.509 (5) Å, b = 12.905 (3) Å, c = 12.051 (3) Å, α = 108.51 (2)°, β = 92.41 (2)°, γ = 89.22 (3)°, and Z = 2. A unit cell contains two independent and nearly identical cluster units A and B. The cluster skeleton is a regular octahedron of six tungsten atoms coordinated with μ_3-sulfido ligands on each triangular face and triethylphosphine on each metal vertex. The structure is almost identical with that of the molybdenum analogue, but the electronic spectra (λ_{max} (ϵ) 409 (8.7×10^3), 882 (2.5×10^3), 964 (sh)) and the one-electron-oxidation (−0.46 V) and -reduction (−1.83 V) potentials vs the ferrocene/ferrocenium (Fc/Fc^+) redox couple in CH_2Cl_2 are significantly different. The difference is discussed in terms of the electronic levels of the W_6S_8 framework, which may be regarded as the cluster core of the unknown tungsten analogues of the Chevrel phases.

Introduction

The superconducting Chevrel phases $M_xMo_6X_8$ (M = Pb, Sn, Cu, etc.; X = S, Se, Te) have been extensively studied,[1] but no tungsten analogue has been reported. It would be very useful to have evidence for the stability of the W_6X_8 cluster framework before starting synthetic efforts on "tungsten Chevrels", and also the electronic properties of the molecular W_6X_8 cluster would give us a clue to the properties of the still unknown solid-state $M_xW_6X_8$ compounds. We report here the synthesis of $[W_6S_8(PEt_3)_6]$ as the second example of reductive dimerization of trinuclear sulfido complexes to form an octahedral cluster.[2] As the potential starting compound $W_3S_7Cl_4$ had not been reported, we first tried to prepare it from tungsten dichloride.[3]

Experimental Section

Reagents. W_6Cl_{12}[4] was prepared by treating $(H_3O)_2[W_6Cl_{14}]\cdot 6H_2O$ under vacuum at 230 °C for 2 h. PEt_3 (21.6% in toluene, Nippon Chemical Co. Ltd.) was used as received. The solvents were dried and distilled under dinitrogen.

Instruments. Infrared spectra were recorded by a Hitachi 295 instrument (4000–250 cm^{-1}). UV-vis spectra were obtained by Simadzu UV-265FS (300–900 nm) and Hitachi U-3400 (900–2000 nm) spectrophotometers. XPS spectra were measured by a VG Scientific Escalab

* To whom correspondence should be addressed at the Department of Chemistry, Faculty of Science, The University of Tokyo, Hongo, Tokyo 113, Japan.
† Osaka University.
‡ Yamagata University.

(1) *Superconductivity in Ternary Compounds I*; Fischer, Ø., Maple, M. B., Eds.; Springer-Verlag: Berlin, 1982.
(2) Saito, T.; Yamamoto, N.; Yamagata, T.; Imoto, H. *J. Am. Chem. Soc.* **1988**, *110*, 1646.
(3) Opalovskii, A. A.; Federov, V. E.; Mazhara, A. P.; Chermisina, I. M. *Zh. Neorg. Khim.* **1972**, *17*, 2876.
(4) Schäfer, H.; Trenkel, M.; Brendel, C. *Monatsh. Chem.* **1971**, *102*, 1293.

0020-1669/89/1328-3588$01.50/0

Table I. Crystallographic Data for $[W_6S_8(P(C_2H_5)_3)_6]$

chem formula	$C_{36}H_{90}P_6S_8W_6$	Z	2
fw	2068.58	T, °C	20
space group	$P\bar{1}$	λ(Mo Kα), Å	0.71069
a, Å	20.509 (5)	ρ_{obsd}, g cm^{-3}	2.267 (8)
b, Å	12.905 (3)	ρ_{calcd}, g cm^{-3}	2.273
c, Å	12.051 (3)	μ, cm^{-1}	120.7
α, deg	108.51 (2)	rel transm factor	1.00–0.365
β, deg	92.41 (2)	$R(F_o)$	0.058
γ, deg	89.22 (3)	$R_w(F_o^2)$	0.060
V, Å^3	3022 (1)		

MkII spectrometer, and the binding energies were calibrated with a C 1s binding energy of 284.6 eV. Powder diffraction data were obtained on a Rigaku RAD-ROC instrument at the X-Ray Diffraction Service of the Department of Chemistry, Faculty of Science, Osaka University.

Synthesis. Heating a mixture of W_6Cl_{12} (1.7 g, 1.1 mmol) and elemental sulfur (1.5 g, 47 mmol) in a sealed Pyrex tube at 300 °C for 20 h, followed by removing excess sulfur and byproducts in vacuo at 280 °C for 3 h, gave a brown solid (**1**). The elemental analysis indicated that the solid product had the composition $W_3S_7Cl_4$. Treatment of **1** (1.5 g) with triethylphosphine (21% toluene solution, 14.0 mL) at room temperature under a dinitrogen atmosphere formed a homogeneous green solution. The solvent was removed under reduced pressure, the residue was redissolved in THF (5.0 mL), and magnesium (0.12 g, 5 mmol) was added. After the mixture was stirred for 48 h at room temperature, the solvent was removed, the residue was washed with acetone, and the products were chromatographed on a Florisil column with dichloromethane. Light brown crystals of $[W_6S_8(PEt_3)_6]$ (**3**) were obtained in 10% yield from the second yellow-brown band. Anal. Calcd for $C_{36}H_{90}P_6S_8W_6$: C, 20.90; H, 4.39; S, 12.40. Found: C, 20.95; H, 4.16; S, 12.64.

X-ray Structure Determination of 3. Single crystals were grown from a dichloromethane–acetone mixed solvent under dinitrogen. A single crystal was fixed on the end of a glass fiber for the X-ray measurements. Approximate cell dimensions and space group were determined from oscillation and Weissenberg photographs, and accurate unit cell dimensions were determined by least-squares refinement with 40 reflections ($20.5° < 2\theta < 27.8°$). Intensity data were collected at 20 °C with a Rigaku AFC-4 four-circle automated diffractometer equipped with a Rotaflex rotating-anode X-ray generator (40 kV, 200 mA) with graphite-monochromatized Mo Kα radiation. No systematic absences exist in the diffraction data. Possible triclinic space groups are the centrosymmetric $P\bar{1}$ and the noncentrosymmetric $P1$. The $P\bar{1}$ possibility was strongly indicated by the number of molecules per unit cell ($Z = 2$) and was confirmed by the successful solution of the structure in this higher symmetry group. The positions of six molybdenum atoms and eight sulfur atoms were determined by direct methods with use of MULTAN78. The remaining non-hydrogen atoms were located on the Fourier maps, and they were refined by the full-matrix least-squares method. Hydrogen atoms were not included in the calculations. Six low-angle reflections (110, −110, 200, 001, −201, −101) were omitted from the final refinement for their extinction. The final residuals are $R = 0.058$ and $R_W = 0.060$. The crystallographic data, experimental information, and structure refinement parameters are given in Table I and in the supplementary material. Atomic coordinates are listed in Table II. All calculations were performed with program libraries on an NEC ACOS S930 computer at the Protein Engineering Research Center, Osaka University.

Electrochemistry. Voltammetric measurements were performed on a HECS-312B polarographic analyzer coupled with a HECS-321B function generator (Huso Co.). A three-electrode cell consisting of a glassy-carbon-disk working electrode (diameter 0.3 cm), a Pt-coil auxiliary electrode, and a saturated sodium calomel reference electrode (SSCE) was employed. The ferrocene/ferrocenium (Fc/Fc^+) redox couple was used as a standard of potential. Thin-layer coulometry was carried out on a HECS-312B polarographic analyzer coupled with a HECS-978 coulometer (Huso Co.), with use of a thin-layer (μm) electrochemical cell with a glassy-carbon disk (diameter 0.3 cm) as a working electrode. Tetrabutylammonium tetrafluoroborate (Nakarai Tesque Inc., specially prepared reagent for polarography) was used as the supporting electrolyte without further purification. Reagent grade dichloromethane (Wako Pure Chemicals Industries) was refluxed over CaH_2 for several hours and then fractionally distilled. Reagent grade tetrahydrofuran (Wako Pure Chemicals Industries) was refluxed over CuCl for 30 min and then purified by fractional distillation.

Results

Synthesis. The reaction of tungsten dichloride and elemental sulfur at 300–320 °C took place smoothly and ended in 20 h. The brown solid product was stable in air, and the elemental analyses of sulfur and chlorine agreed with the composition $W_3S_7Cl_4$ (**1**).[5] When heated at 320–380 °C, it changed, by releasing sulfur, into a solid with the composition $W_3S_4Cl_4$ (**2**),[7] which no longer reacted

Table II. Fractional Atomic Coordinates and Equivalent Isotropic Thermal Parameters for $[W_6S_8(PEt_3)_6]$[a]

atom	x	y	z	$U_{eq/iso}$, Å^2
W(11)	−0.01014 (5)	0.09784 (9)	−0.08824 (11)	0.0324 (4)
W(12)	−0.06131 (5)	0.08198 (9)	0.10672 (11)	0.0329 (4)
W(13)	0.06847 (5)	0.08762 (9)	0.09141 (11)	0.0311 (4)
S(11)	−0.0024 (3)	0.2455 (6)	0.0998 (8)	0.048 (3)
S(12)	0.0155 (3)	0.0655 (6)	0.2612 (7)	0.043 (3)
S(13)	−0.1285 (3)	0.0845 (6)	−0.0639 (7)	0.042 (3)
S(14)	0.1096 (3)	0.0943 (6)	−0.0960 (7)	0.042 (3)
P(11)	−0.0243 (4)	0.2319 (6)	−0.2012 (7)	0.047 (3)
P(12)	−0.1425 (3)	0.1891 (7)	0.2511 (8)	0.049 (3)
P(13)	0.1567 (3)	0.2055 (6)	0.2203 (7)	0.047 (3)
W(21)	0.50971 (5)	0.60028 (10)	−0.08377 (12)	0.0391 (5)
W(22)	0.43724 (5)	0.59276 (10)	0.09334 (12)	0.0390 (5)
W(23)	0.56730 (5)	0.57186 (10)	0.10871 (12)	0.0399 (5)
S(21)	0.6286 (3)	0.5737 (6)	−0.0609 (7)	0.045 (3)
S(22)	0.4944 (3)	0.5593 (7)	0.2602 (8)	0.049 (3)
S(23)	0.5123 (3)	0.7434 (7)	0.1092 (8)	0.053 (4)
S(24)	0.3893 (3)	0.6111 (6)	−0.0912 (8)	0.050 (3)
P(21)	0.5209 (4)	0.7342 (7)	−0.1957 (8)	0.054 (3)
P(22)	0.3559 (4)	0.7160 (7)	0.2243 (8)	0.058 (4)
P(23)	0.6587 (4)	0.6647 (8)	0.2482 (9)	0.068 (4)
C(1)	−0.016 (1)	0.174 (2)	−0.362 (3)	0.057 (8)
C(2)	0.050 (1)	0.133 (3)	−0.395 (3)	0.078 (10)
C(3)	−0.104 (1)	0.296 (3)	−0.198 (3)	0.071 (9)
C(4)	−0.122 (1)	0.366 (3)	−0.070 (3)	0.075 (10)
C(5)	0.034 (1)	0.348 (3)	−0.152 (3)	0.067 (9)
C(6)	0.031 (2)	0.431 (3)	−0.227 (4)	0.087 (11)
C(7)	−0.147 (2)	0.133 (3)	0.374 (4)	0.108 (14)
C(8)	−0.193 (2)	0.199 (4)	0.472 (5)	0.133 (17)
C(9)	−0.125 (2)	0.339 (3)	0.317 (4)	0.093 (12)
C(10)	−0.059 (2)	0.354 (3)	0.398 (3)	0.082 (10)
C(11)	−0.225 (2)	0.206 (3)	0.198 (4)	0.092 (12)
C(12)	−0.259 (2)	0.087 (4)	0.157 (5)	0.144 (18)
C(13)	0.123 (1)	0.308 (3)	0.347 (3)	0.067 (9)
C(14)	0.178 (2)	0.383 (4)	0.435 (5)	0.126 (16)
C(15)	0.222 (1)	0.134 (2)	0.280 (3)	0.059 (8)
C(16)	0.192 (1)	0.074 (3)	0.363 (3)	0.070 (9)
C(17)	0.209 (1)	0.280 (3)	0.152 (3)	0.067 (9)
C(18)	0.171 (2)	0.370 (3)	0.114 (3)	0.084 (11)
C(19)	0.508 (2)	0.667 (3)	−0.367 (4)	0.109 (14)
C(20)	0.433 (2)	0.638 (4)	−0.394 (4)	0.111 (14)
C(21)	0.602 (1)	0.791 (3)	−0.192 (3)	0.073 (9)
C(22)	0.625 (1)	0.860 (3)	−0.067 (3)	0.077 (10)
C(23)	0.463 (1)	0.852 (3)	−0.144 (3)	0.079 (10)
C(24)	0.467 (2)	0.937 (4)	−0.224 (4)	0.114 (14)
C(25)	0.397 (2)	0.812 (3)	0.356 (4)	0.106 (13)
C(26)	0.348 (3)	0.879 (5)	0.446 (6)	0.185 (23)
C(27)	0.301 (2)	0.799 (3)	0.160 (3)	0.079 (10)
C(28)	0.342 (2)	0.885 (4)	0.129 (4)	0.124 (15)
C(29)	0.288 (1)	0.643 (3)	0.268 (3)	0.075 (9)
C(30)	0.316 (2)	0.574 (3)	0.348 (4)	0.108 (13)
C(31)	0.641 (2)	0.719 (4)	0.405 (4)	0.118 (15)
C(32)	0.588 (2)	0.812 (4)	0.411 (5)	0.131 (16)
C(33)	0.694 (2)	0.777 (4)	0.210 (4)	0.114 (14)
C(34)	0.761 (2)	0.828 (5)	0.290 (6)	0.171 (21)
C(35)	0.726 (2)	0.570 (4)	0.263 (4)	0.119 (15)
C(36)	0.766 (2)	0.529 (4)	0.149 (5)	0.138 (17)

[a] Carbon atoms were refined isotropically. Anisotropically refined atoms are given isotropic equivalent thermal parameters defined as $U_{eq} = {}^1/_3\sum_i\sum_j U_{ij}a_i^*a_j^*\mathbf{a}_i\cdot\mathbf{a}_j$.

(5) The powder X-ray diffraction spectrum showed broad lines, and the pattern resembled the calculated one for the hypothetical $W_3S_7Cl_4$ with the same atomic and cell parameters as $Mo_3S_7Cl_4$.[6] However, we have so far not achieved the complete fitting of the calculated pattern by adjusting the cell parameters.

(6) Marcoll, J.; Rabenau, A.; Mootz, D.; Wunderlich, H. *Rev. Chim. Miner.* **1974**, *11*, 607.

(7) The powder pattern (Table VIII in the supplementary material) could be indexed with a rhombohedral symmetry ($a = 11.560$ (2) Å, $c = 7.319$ (2) Å in the hexagonal setting).

Table III. Interatomic Distances (Å) and Angles (deg) and Esd Values for $[W_6S_8(PEt_3)_6]$

W(11)–W(12)	2.680 (2)	W(11)–W(13)	2.681 (2)	W(12)–P(12)	2.52 (1)	W(13)–P(13)	2.518 (8)
W(11)–W(11)′	3.792 (2)	W(11)–W(12)′	2.681 (2)	P(11)–C(1)	1.86 (3)	P(11)–C(3)	1.81 (3)
W(11)–W(13)′	2.679 (2)	W(12)–W(13)	2.679 (2)	P(11)–C(5)	1.85 (3)	P(12)–C(7)	1.85 (4)
W(12)–W(12)′	3.790 (2)	W(12)–W(13)′	2.678 (2)	P(12)–C(9)	1.88 (4)	P(12)–C(11)	1.82 (4)
W(13)–W(13)′	3.788 (2)	W(11)–S(11)	2.455 (8)	P(13)–C(13)	1.83 (3)	P(13)–C(15)	1.86 (3)
W(11)–S(13)	2.47 (1)	W(11)–S(14)	2.460 (7)	P(13)–C(17)	1.83 (3)	C(1)–C(2)	1.48 (5)
W(11)–S(12)′	2.45 (1)	W(12)–S(11)	2.472 (8)	C(3)–C(4)	1.58 (5)	C(5)–C(6)	1.60 (5)
W(12)–S(12)	2.45 (1)	W(12)–S(13)	2.436 (7)	C(7)–C(8)	1.56 (7)	C(9)–C(10)	1.61 (5)
W(12)–S(14)′	2.46 (1)	W(13)–S(11)	2.464 (8)	C(11)–C(12)	1.61 (6)	C(13)–C(14)	1.60 (6)
W(13)–S(12)	2.45 (1)	W(13)–S(14)	2.470 (7)	C(15)–C(16)	1.59 (4)	C(17)–C(18)	1.56 (5)
W(13)–S(13)′	2.46 (1)	W(11)–P(11)	2.525 (8)				
W(21)–W(22)	2.679 (2)	W(21)–W(23)	2.685 (2)	W(22)–P(22)	2.522 (9)	W(23)–P(23)	2.51 (1)
W(21)–W(21)′	3.788 (2)	W(21)–W(22)′	2.675 (2)	P(21)–C(19)	1.97 (4)	P(21)–C(21)	1.82 (4)
W(21)–W(23)′	2.674 (2)	W(22)–W(23)	2.682 (2)	P(21)–C(23)	1.87 (4)	P(22)–C(25)	1.85 (4)
W(22)–W(22)′	3.784 (2)	W(22)–W(23)′	2.674 (2)	P(22)–C(27)	1.85 (4)	P(22)–C(29)	1.87 (4)
W(23)–W(23)′	3.791 (2)	W(21)–S(21)	2.475 (7)	P(23)–C(31)	1.84 (5)	P(23)–C(33)	1.82 (5)
W(21)–S(23)	2.47 (1)	W(21)–S(24)	2.471 (8)	P(23)–C(35)	1.88 (5)	C(19)–C(20)	1.59 (6)
W(21)–S(22)′	2.45 (1)	W(22)–S(22)	2.438 (8)	C(21)–C(22)	1.54 (5)	C(23)–C(24)	1.68 (6)
W(22)–S(23)	2.45 (1)	W(22)–S(24)	2.472 (8)	C(25)–C(26)	1.56 (8)	C(27)–C(28)	1.54 (6)
W(22)–S(21)′	2.47 (1)	W(23)–S(21)	2.452 (7)	C(29)–C(30)	1.59 (5)	C(31)–C(32)	1.59 (7)
W(23)–S(22)	2.45 (1)	W(23)–S(23)	2.470 (9)	C(33)–C(34)	1.65 (7)	C(35)–C(36)	1.57 (7)
W(23)–S(24)′	2.46 (1)	W(21)–P(21)	2.524 (9)				

W(12)–W(11)–W(13)	59.98 (4)	W(12)–W(11)–W(12)′	89.96 (5)	W(12)–W(13)–S(12)	56.7 (2)	W(12)–W(13)–S(14)	116.8 (2)
W(12)–W(11)–W(13)′	59.98 (4)	W(13)–W(11)–W(12)′	59.94 (4)	W(12)–W(13)–S(13)′	117.3 (2)	W(12)–W(13)–P(13)	132.9 (2)
W(13)–W(11)–W(13)′	89.93 (5)	W(12)′–W(11)–W(13)′	59.98 (4)	W(11)′–W(13)–S(11)	117.3 (2)	W(11)′–W(13)–S(12)	56.8 (2)
W(11)–W(12)–W(13)	60.02 (4)	W(11)–W(12)–W(11)′	90.04 (5)	W(11)′–W(13)–S(14)	116.8 (2)	W(11)′–W(13)–S(13)′	57.3 (2)
W(11)–W(12)–W(13)′	59.99 (4)	W(13)–W(12)–W(11)′	59.97 (4)	W(11)′–W(13)–P(13)	133.8 (2)	W(12)′–W(13)–S(11)	116.8 (2)
W(13)–W(12)–W(13)′	89.97 (5)	W(11)′–W(12)–W(13)′	60.02 (4)	W(12)′–W(13)–S(12)	116.8 (2)	W(12)′–W(13)–S(14)	56.8 (2)
W(11)–W(13)–W(12)	60.00 (4)	W(11)–W(13)–W(11)′	90.07 (5)	W(12)′–W(13)–S(13)′	56.4 (2)	W(12)′–W(13)–P(13)	137.1 (2)
W(11)–W(13)–W(12)′	60.04 (4)	W(12)–W(13)–W(11)′	60.05 (4)	S(11)–W(11)–S(13)	89.4 (3)	S(11)–W(11)–S(14)	89.9 (3)
W(12)–W(13)–W(12)′	90.03 (5)	W(11)′–W(13)–W(12)′	60.03 (4)	S(11)–W(11)–S(12)′	172.6 (3)	S(11)–W(11)–P(11)	92.1 (3)
W(12)–W(11)–S(11)	57.4 (2)	W(12)–W(11)–S(13)	56.3 (2)	S(13)–W(11)–S(14)	172.1 (2)	S(13)–W(11)–S(12)′	90.4 (3)
W(12)–W(11)–S(14)	117.2 (2)	W(12)–W(11)–S(12)′	116.8 (2)	S(13)–W(11)–P(11)	93.8 (3)	S(14)–W(11)–S(12)′	89.3 (3)
W(12)–W(11)–P(11)	133.8 (2)	W(13)–W(11)–S(11)	57.2 (2)	S(14)–W(11)–P(11)	94.1 (3)	S(12)′–W(11)–P(11)	95.3 (3)
W(13)–W(11)–S(13)	116.2 (2)	W(13)–W(11)–S(14)	57.2 (2)	S(11)–W(12)–S(12)	90.0 (3)	S(11)–W(12)–S(13)	89.9 (3)
W(13)–W(11)–S(12)′	116.6 (2)	W(13)–W(11)–P(11)	134.4 (2)	S(11)–W(12)–S(14)′	172.6 (3)	S(11)–W(12)–P(12)	94.5 (3)
W(12)′–W(11)–S(11)	117.1 (2)	W(12)′–W(11)–S(13)	116.8 (2)	S(12)–W(12)–S(13)	173.0 (3)	S(12)–W(12)–S(14)′	89.5 (3)
W(12′)–W(11)–S(14)	56.9 (2)	W(12)′–W(11)–S(12)′	56.8 (2)	S(12)–W(12)–P(12)	93.1 (3)	S(13)–W(12)–S(14)′	89.8 (2)
W(12)′–W(11)–P(11)	136.3 (2)	W(13)′–W(11)–S(11)	117.3 (2)	S(13)–W(12)–P(12)	93.9 (3)	S(14)′–W(12)–P(12)	92.9 (3)
W(13)′–W(11)–S(13)	56.9 (2)	W(13)′–W(11)–S(14)	116.8 (2)	S(11)–W(13)–S(12)	90.0 (3)	S(11)–W(13)–S(14)	89.4 (3)
W(13)′–W(11)–S(12)′	56.9 (2)	W(13)′–W(11)–P(11)	135.7 (2)	S(11)–W(13)–S(13)′	172.4 (3)	S(11)–W(13)–P(13)	92.9 (3)
W(11)–W(12)–S(11)	56.8 (2)	W(11)–W(12)–S(12)	116.9 (2)	S(12)–W(13)–S(14)	172.1 (3)	S(12)–W(13)–S(13)′	90.6 (3)
W(11)–W(12)–S(13)	57.6 (2)	W(11)–W(12)–S(14)′	117.3 (2)	S(12)–W(13)–P(13)	91.7 (3)	S(14)–W(13)–S(13)′	88.9 (2)
W(11)–W(12)–P(12)	136.0 (2)	W(13)–W(12)–S(11)	57.0 (2)	S(14)–W(13)–P(13)	96.2 (3)	S(13)′–W(13)–P(13)	94.6 (3)
W(13)–W(12)–S(12)	56.9 (2)	W(13)–W(12)–S(13)	117.6 (2)	W(11)–P(11)–C(1)	116 (1)	W(11)–P(11)–C(3)	117 (1)
W(13)–W(12)–S(14)′	117.0 (2)	W(13)–W(12)–P(12)	134.9 (2)	W(11)–P(11)–C(5)	113 (1)	W(12)–P(12)–C(7)	110 (1)
W(11)′–W(12)–S(11)	116.9 (2)	W(11)′–W(12)–S(12)	56.8 (2)	W(12)–P(12)–C(9)	115 (1)	W(12)–P(12)–C(11)	119 (1)
W(11)′–W(12)–S(13)	117.3 (2)	W(11)′–W(12)–S(14)′	57.0 (2)	W(13)–P(13)–C(13)	112 (1)	W(13)–P(13)–C(15)	117 (1)
W(11)′–W(12)–P(12)	134.0 (2)	W(13)′–W(12)–S(11)	116.7 (2)	W(13)–P(13)–C(17)	117 (1)	P(11)–C(1)–C(2)	113 (2)
W(13)′–W(12)–S(12)	116.8 (2)	W(13)′–W(12)–S(13)	57.3 (2)	P(11)–C(3)–C(4)	113 (2)	P(11)–C(5)–C(6)	116 (2)
W(13)′–W(12)–S(14)′	57.3 (2)	W(13)′–W(12)–P(12)	135.1 (2)	P(12)–C(7)–C(8)	114 (3)	P(12)–C(9)–C(10)	109 (2)
W(11)–W(13)–S(11)	56.8 (2)	W(11)–W(13)–S(12)	116.7 (2)	P(12)–C(11)–C(12)	107 (3)	P(13)–C(13)–C(14)	114 (3)
W(11)–W(13)–S(14)	56.9 (2)	W(11)–W(13)–S(13)′	116.4 (2)	P(13)–C(15)–C(16)	111 (2)	P(13)–C(17)–C(18)	113 (2)
W(11)–W(13)–P(13)	136.0 (2)	W(12)–W(13)–S(11)	57.3 (2)				

W(21)–W(22)–W(23)′	59.94 (5)	W(23)–W(22)–W(21)′	59.89 (5)	W(23)′–W(22)–S(23)	117.2 (2)	W(23)′–W(22)–S(24)	57.0 (2)
W(23)–W(22)–W(23)′	90.10 (5)	W(21)′–W(22)–S(23)′	60.24 (5)	W(23)′–W(22)–S(21)′	56.8 (2)	W(23)′–W(22)–P(22)	136.5 (2)
W(21)–W(23)–W(22)	59.89 (5)	W(21)–W(23)–W(21)′	89.95 (5)	W(21)–W(23)–S(21)	57.4 (2)	W(21)–W(23)–S(22)	116.3 (2)
W(21)–W(23)–W(22)′	59.89 (5)	W(22)–W(23)–W(21)′	59.93 (5)	W(21)–W(23)–S(23)	57.0 (2)	W(21)–W(23)–S(24)′	117.2 (2)
W(22)–W(23)–W(22)′	89.0 (5)	W(21)′–W(23)–W(22)′	60.11 (5)	W(21)–W(23)–P(23)	134.6 (2)	W(22)–W(23)–S(21)	117.2 (2)
W(22)–W(21)–S(21)	116.5 (2)	W(22)–W(21)–S(23)	56.7 (2)	W(22)–W(23)–S(22)	56.5 (2)	W(22)–W(23)–S(23)	56.6 (2)
W(22)–W(21)–S(24)	57.2 (2)	W(22)–W(21)–S(22)′	116.9 (2)	W(22)–W(23)–S(24)′	117.2 (2)	W(22)–W(23)–P(23)	136.7 (2)
W(22)–W(21)–P(21)	134.5 (2)	W(23)–W(21)–S(21)	56.6 (2)	W(21)′–W(23)–S(21)	117.5 (2)	W(21)′–W(23)–S(22)	56.8 (2)
W(23)–W(21)–S(23)	57.1 (2)	W(23)–W(21)–S(24)	117.2 (2)	W(21)′–W(23)–S(23)	116.5 (2)	W(21)′–W(23)–S(24)′	57.4 (2)
W(23)–W(21)–S(22)′	116.5 (2)	W(23)–W(21)–P(21)	135.7 (2)	W(21)′–W(23)–P(23)	135.4 (2)	W(22)′–W(23)–S(21)	57.4 (2)
W(22)′–W(21)–S(21)	57.1 (2)	W(22)′–W(21)–S(23)	116.9 (2)	W(22)′–W(23)–S(22)	116.8 (2)	W(22)′–W(23)–S(23)	116.9 (2)
W(22)′–W(21)–S(24)	117.1 (2)	W(22)′–W(21)–S(22)′	56.6 (2)	W(22)′–W(23)–S(24)′	57.4 (2)	W(22)′–W(23)–P(23)	133.4 (2)
W(22)′–W(21)–P(21)	135.6 (2)	W(23)′–W(21)–S(21)	117.3 (2)	S(21)–W(21)–S(23)	89.5 (3)	S(21)–W(21)–S(24)	172.6 (3)
W(23)′–W(21)–S(23)	116.6 (2)	W(23)′–W(21)–S(24)	57.0 (2)	S(21)–W(21)–S(22)′	89.9 (3)	S(21)–W(21)–P(21)	94.7 (3)
W(23)′–W(21)–S(22)′	57.0 (2)	W(23)′–W(21)–P(21)	134.3 (2)	S(23)–W(21)–S(24)	89.5 (3)	S(23)–W(21)–S(22)′	172.1 (3)
W(21)–W(22)–S(22)	117.1 (2)	W(21)–W(22)–S(23)	57.3 (2)	S(23)–W(21)–P(21)	94.0 (3)	S(24)–W(21)–S(22)′	90.0 (3)
W(21)–W(22)–S(24)	57.2 (2)	W(21)–W(22)–S(21)′	116.7 (2)	S(24)–W(21)–P(21)	92.7 (3)	S(22)′–W(21)–P(21)	93.3 (3)
W(21)–W(22)–P(22)	136.3 (2)	W(23)–W(22)–S(22)	57.0 (2)	S(22)–W(22)–S(23)	89.8 (3)	S(22)–W(22)–S(24)	172.8 (3)
W(23)–W(22)–S(23)	57.3 (2)	W(23)–W(22)–S(24)	117.2 (2)	S(22)–W(22)–S(21)′	90.2 (3)	S(22)–W(22)–P(22)	91.6 (3)
W(23)–W(22)–S(21)′	117.2 (2)	W(23)–W(22)–P(22)	133.4 (2)	S(23)–W(22)–S(24)	89.9 (3)	S(23)–W(22)–S(21)′	172.9 (3)
W(21)′–W(22)–S(22)	56.9 (2)	W(21)′–W(22)–S(23)	117.2 (2)	S(23)–W(22)–P(22)	93.2 (3)	S(24)–W(22)–S(21)′	89.2 (3)
W(21)′–W(22)–S(24)	117.2 (2)	W(21)′–W(22)–S(21)′	57.3 (2)	S(24)–W(22)–P(22)	95.6 (3)	S(21)′–W(22)–P(22)	93.9 (3)
W(21)′–W(22)–P(22)	133.6 (2)	W(23)′–W(22)–S(22)	117.1 (2)	S(21)–W(23)–S(22)	172.6 (3)	S(21)–W(23)–S(23)	90.0 (3)

Table III (Continued)

S(21)-W(23)-S(24)′	89.9 (3)	S(21)-W(23)-P(23)	91.8 (3)	W(23)-P(23)-C(31)	118 (1)	W(23)-P(23)-C(33)	113 (1)
S(22)-W(23)-S(23)	89.0 (3)	S(22)-W(23)-S(24)′	90.1 (3)	W(23)-P(23)-C(35)	114 (1)	P(21)-C(19)-C(20)	108 (3)
S(22)-W(23)-P(23)	95.6 (3)	S(23)-W(23)-S(24)′	172.7 (3)	P(21)-C(21)-C(22)	112 (2)	P(21)-C(23)-C(24)	112 (2)
S(23)-W(23)-P(23)	94.8 (3)	S(24)′-W(23)-P(23)	92.5 (3)	P(22)-C(25)-C(26)	113 (3)	P(22)-C(27)-C(28)	110 (3)
W(21)-P(21)-C(19)	113 (1)	W(21)-P(21)-C(21)	116 (1)	P(22)-C(29)-C(30)	111 (2)	P(23)-C(31)-C(32)	104 (3)
W(21)-P(21)-C(23)	112 (1)	W(22)-P(22)-C(25)	111 (1)	P(23)-C(33)-C(34)	114 (3)	P(23)-C(35)-C(36)	111 (3)
W(22)-P(22)-C(27)	118 (1)	W(22)-P(22)-C(29)	115 (1)				

[a] The primes indicate the symmetry operation $-x, -y, -z$.

Table IV. XPS and UV Data for Complexes **3** and **4**

	binding energy, eV[a]				λ_{max}, nm[b] (ϵ, M^{-1} cm^{-1})		
	W $4f_{7/2}$	Mo $3d_{5/2}$, $3d_{3/2}$	S 2p	P 2p			
$[W_5S_8(PEt_3)_6]$	31.2		161.4 162.2 (sh)	130.8	409 (8.7×10^3)	882 (2.5×10^3)	964 sh
$[Mo_6S_8(PEt_3)_6]$		227.8 231.0	161.1 162.1 (sh)	130.6	491 (8.1×10^3)	991 (1.2×10^3)	1200 sh

[a] C 1s binding energy 284.6 eV. [b] **3** in chloroform solution; **4** in benzene solution.

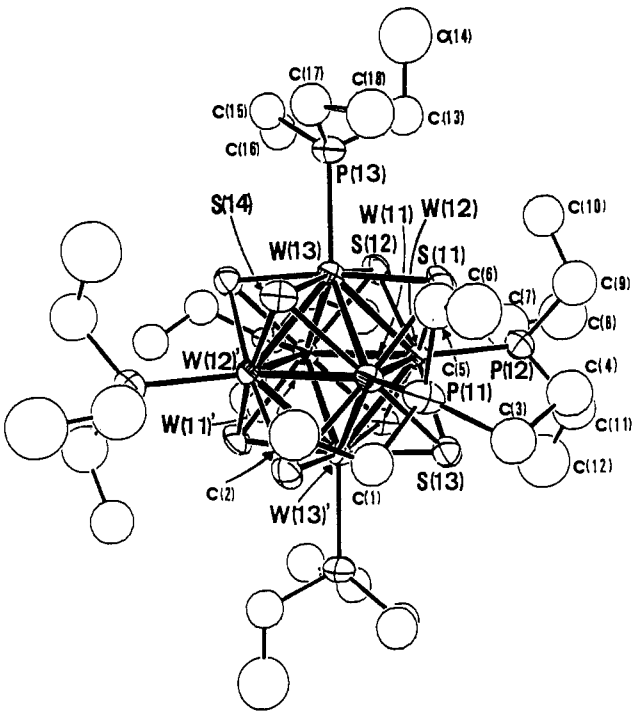

Figure 1. Molecular structure of $[W_6S_8(PEt_3)_6]$ (**3A**) with the numbering scheme of atoms shown (ORTEP). The thermal ellipsoids are drawn at the 50% probability level.

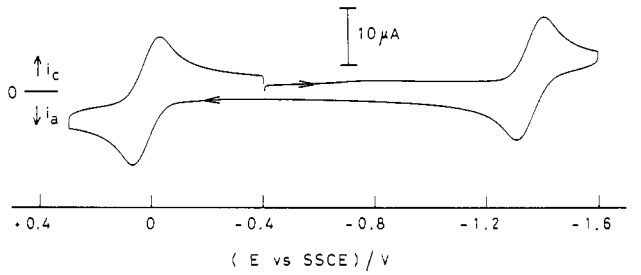

Figure 2. Cyclic voltammogram of 0.5 mM $[W_6S_8(PEt_3)_6]$ at a glassy-carbon electrode in a CH_2Cl_2 solution containing 0.1 M $(NBu_4)BF_4$ (scan rate 0.2 V s^{-1}).

Table V. Formal Potentials for Complexes **3** and **4**[a]

	solvent	$E°$, V vs Fc/Fc^+ 1+/0	$E°$, V vs Fc/Fc^+ 0/1−
$[W_6S_8(PEt_3)_6]$	CH_2Cl_2	−0.46	−1.83
	THF	−0.34	−1.86
$[Mo_6S_8(PEt_3)_6]$	CH_2Cl_2	−0.24	−1.51
	THF	−0.09	−1.54

[a] $E°(Fc/Fc^+)$ = 0.483 V (in CH_2Cl_2) and 0.603 V (in THF) vs SSCE.

with triethylphosphine. It is therefore imperative to carry out the reaction of tungsten dichloride with sulfur under 320 °C. Reaction of the compound **1** with triethylphosphine gave a complex that was soluble in organic solvents. Although we have obtained no analytically pure compound yet, the infrared spectra and electronic spectra (315, 589 nm)[8] suggest that this is a trinuclear tungsten sulfido cluster coordinated with triethylphosphine similar to the molybdenum clusters.[9] The reaction products of the complex with magnesium contain a few products other than **3**. As the hexanuclear cluster **3** is soluble in dichloromethane but insoluble in acetone, washing with acetone could remove the byproducts, and the column chromatography of the dichloromethane solution facilitated the purification of **3**, which is stable in air.

Structure. The space group is $P\bar{1}$, and there are two independent molecules in a unit cell. The selected interatomic distances and angles are listed in Table III. As little difference exists between the structures of the two molecules, only one of them (A) is illustrated in Figure 1. Six tungsten atoms form an almost regular octahedron, and the W–W single-bond distances range from 2.6782 (9) to 2.6808 (9) Å in A and from 2.6727 (9) to 2.6851 (9) Å in B. The W–W–W angles are very near 60 and 90°. Eight sulfur atoms cap the W_3 faces of the W_6 octahedron, and a triethylphosphine ligand coordinates to each tungsten atom. The W–μ_3-S distance (average) is 2.458 Å, and the tungsten atoms slightly emerge from the cube composed of the eight sulfur atoms.

Spectra. The peak positions of the electronic spectra and X-ray photoelectron spectra are shown in Table IV, together with the corresponding values for the molybdenum analogue. The bands in the electronic spectra of the tungsten cluster **3** shift to considerably shorter wavelengths, but the S 2p and P 2p binding energies of the compound are only slightly larger than those of the molybdenum cluster **4**.

Electrochemistry. The typical cyclic voltammogram of a 0.5 mM dichloromethane solution of **3** containing 0.1 M $(Bu_4N)BF_4$ (Figure 2) exhibits both reversible reduction and reversible oxidation.[10] The values of i_{pa}/i_{pc} for reduction and i_{pc}/i_{pa} for oxidation are unity at the scan rates of 0.02–0.20 V s^{-1}. On the basis

(8) (a) Shibahara, T.; Kohda, K.; Ohtsuji, A.; Yasuda, K.; Kuroya, H. *J. Am. Chem. Soc.* **1986**, *108*, 2757. (b) Cotton, F. A.; Llusar, R. *Inorg. Chem.* **1988**, *27*, 1303.

(9) Saito, T.; Yamamoto, N.; Yamagata, T.; Imoto, H. *Chem. Lett.* **1987**, 2025.

(10) Although the molybdenum cluster **4** showed a second reduction wave at −2.51 V vs Fc/Fc^+ in a THF solution, it was impossible to observe a similar wave for the tungsten cluster **3**, due probably to the limit of the "window" of THF. Saito, T.; Unoura, K. To be submitted for publication.

of the result of the thin-layer coulometry, the number of electrons concerned with reduction and oxidation is 1. These results indicate that the cluster **3** undergoes one-electron reversible reduction and one-electron reversible oxidation in dichloromethane. The voltammetric behavior of **3** in THF is very similar to that in dichloromethane. Accordingly, the electrochemical processes are expressed as

$$[W_6S_8(PEt_3)_6]^+ \underset{-e^-}{\overset{+e^-}{\rightleftharpoons}} [W_6S_8(PEt_3)_6] \underset{-e^-}{\overset{+e^-}{\rightleftharpoons}} [W_6S_8(PEt_3)_6]^-$$

The formal potentials for **3** vs the Fc/Fc^+ redox couple are given in Table V.

Discussion

Synthesis. As the intermediate trinuclear complex has not been fully characterized and the yield of the hexanuclear complex **3** is rather low, the pathway of the formation of **3** is not clear at present. However, it is likely that the hexanuclear cluster complex is formed by reductive dimerization of two trinuclear cluster complexes.[2]

Structure. The cluster complex **3** is the first example of a compound with the W_6S_8 cluster framework. Neither solid compounds nor molecular complexes with this cluster unit are known,[11] but the structural features of **3** are almost identical with those of the molybdenum analogue.[2] Just like the molybdenum complex, the 20-electron tungsten cluster complex is free from strong intercluster interactions and has a regular octahedral cluster skeleton. Although the molecular orbital calculation of the W_6S_8 clusters has not been reported, the basic level scheme should be similar to that of the Mo_6S_8 clusters;[12] namely, the HOMO is either the triply degenerate t_{2u} or t_{1u} and the LUMO is doubly degenerate e_g. The undistorted octahedron of the cluster implies that the HOMO is just occupied with 20 electrons.

The W-W bond distance (average) of 2.678 Å in **3** is slightly longer than that in the 24e cluster complex $[W_6Cl_{12}(PBu_3)_2]$ (**5**) (average) of 2.626 Å.[13] The longer distance can be interpreted in terms of a larger electrostatic repulsion between the tungsten atoms in the 16/6 oxidation state as compared with 12/6 in **5**. The average W-W bond distance in **3** is slightly longer than the Mo-Mo distance in the molybdenum analogue **4** (2.663 Å). A similar trend has been observed in the 24e cluster complexes $[M_6Cl_{12}(PBu_3)_2]$ (M = Mo, W).[13,14]

Orbital Energy Levels and Electron Transfer. Although the whole structure is almost identical with that of the molybdenum analogue, the tungsten cluster is significantly different in the electronic properties. The electrochemical reduction and oxidation potentials of the compound are related to the LUMO and HOMO energy levels, respectively.[15] The energy difference of the cathodic and anodic processes approximates the energy difference of the frontier orbitals. The energy difference is 1.37 eV for the dichloromethane solution and 1.52 eV for the THF solution of the cluster **3**. Corresponding values for the molybdenum cluster are 1.27 and 1.45 eV. Therefore, the energy differences for the tungsten cluster **3** are about 0.1 eV larger in both solvents. The main bands of the electronic spectra at longer wavelengths (882 nm (1.40 eV) for **3** and 991 nm (1.25 eV) for **4**)[2] are probably the transitions between the HOMO and LUMO. The values are near those of the electrochemistry in dichloromethane. The nature of the solvent effects is not clear at present. The molecular orbital calculations for the Mo_6S_8 systems have shown that the energy difference between the HOMO (t_{2u} or t_{1u}) and the LUMO (e_g) is about 1 eV.[12] As the redox potentials should reflect the involved orbital energies, the frontier orbitals of the tungsten complex are at a level about 0.2-0.3 eV higher than those of the molybdenum analogue. This energy difference in the molecular clusters $[M_6S_8(PEt_3)_6]$ (M = Mo, W) would also remain in the solid-state M_6S_8 compounds and affect the conductivity properties. We anticipate the synthesis of the solid-state tungsten cluster compounds with W_6S_8 cluster units.

Acknowledgment. The support from the Ministry of Education, Science and Culture of Japan (Grant-in-Aid for General Research No. 63430010) and the gift of triethylphosphine from Nippon Chemical Co. Ltd. are gratefully acknowledged. The XPS spectra were measured at the Coordination Chemistry Laboratories of the Institute for Molecular Science under the Cooperative Research Program.

Supplementary Material Available: Listings of anisotropic thermal parameters, powder diffraction data for **2**, and complete crystal data for **3** (4 pages); a listing of calculated and observed structure factors for **3** (14 pages). Ordering information is given on any current masthead page.

(11) Yvon, K. In ref 1, p 90.
(12) (a) Le Beuze, L.; Makhyoun, M. A.; Lissillour, R.; Chermette, H. *J. Chem. Phys.* **1982**, *76*, 6060. (b) Hughbanks, T.; Hoffmann, R. *J. Am. Chem. Soc.* **1983**, *105*, 1150. (c) Burdett, J. K.; Lin, J. H. *Inorg. Chem.* **1982**, *21*, 5. (d) Imoto, H.; Saito, T.; Adachi, H. To be submitted for publication.
(13) Saito, T.; Manabe, H.; Yamagata, T.; Imoto, H. *Inorg. Chem.* **1987**, *26*, 1362.
(14) Saito, T.; Nishida, M.; Yamagata, T.; Yamagata, Y.; Yamaguchi, Y. *Inorg. Chem.* **1986**, *25*, 1111.
(15) Lemoine, P. *Coord. Chem. Rev.* **1988**, *83*, 169.

Contribution from the Institute of Inorganic Synthesis, Yamanashi University, Miyamae-cho 7, Kofu 400, Japan

A New Lithium Insertion Compound, $(Li,Cu)TaO_3$, with the $LiNbO_3$ Type Structure

Nobuhiro Kumada,* Satoru Hosoda, Fumio Muto, and Nobukazu Kinomura

Received November 28, 1988

A new lithium insertion compound, $(Li,Cu)TaO_3$, was prepared from $CuTa_2O_6$ by chemical reaction with *n*-butyllithium. The lithium insertion reaction was accompanied by a topotactic transformation from the perovskite-related structure to the $LiNbO_3$ type structure. The hexagonal lattice parameters of the compound are $a = 5.176$ (2) and $c = 13.81$ (1) Å. The structure was refined by the X-ray powder Rietveld method; reliability factors are $R_{wP} = 5.7$, $R_P = 4.5$, and $R_B = 7.4\%$. The cation arrangement of $(Li,Cu)TaO_3$ is similar to that of $LiTaO_3$ rather than to that of the high-pressure form of $CuTaO_3$.

Introduction

Lithium insertion (lithiation) has been investigated on various transition-metal oxides by chemical or electrochemical methods. Lithiation is an important secondary battery cathode reaction and has been extended to syntheses of new compounds, as seen, for example, in the lithiation of ReO_3,[1] rutile,[2] and spinel[3-5] type oxides. These oxides have cavities or tunnels available to incorporate the lithium ions. In many cases the oxygen array of

(1) Cava, R. J.; Santoro, A.; Murphy, D. W.; Zahurak, S.; Roth, R. S. *J. Solid State Chem.* **1982**, *42*, 251.
(2) Murphy, D. W.; Di Salvo, F. J.; Waszczak, J. N. *Mater. Res. Bull.* **1978**, *13*, 1395.
(3) Chen, C. J.; Greenblatt, M. *Solid State Ionics* **1986**, *18&19*, 838.
(4) Chen, C. J.; Greenblatt, M.; Waszczak, J. V. *J. Solid State Chem.* **1986**, *64*, 240.
(5) Thackeray, M. M.; David, W. I. F.; Bruce, P. G.; Goodenough, J. B. *Mater. Res. Bull.* **1983**, *18*, 461.

0020-1669/89/1328-3592$01.50/0